Supplementary Information for

Synergistic integration of FeNi magnetic nanoparticles with graphene-based porous carbon for efficient capture of N-linked glycans

Yang Wang, [1, a] Jiaxi Wang, [1, a] Jie Li, [1] Yun Ling, [1,2,*] Yu Jia, [1] Yongtai Yang, [1] Xiaofeng Liu, [1] Xiangmin Zhang, [1] Yaming Zhou [1,*]

[1] Shanghai Key Laboratory of Molecular Catalysis and Innovative Materials, Department of Chemistry, Fudan University, Shanghai, 200438, China.

[2] Zhuhai-Fudan Innovation Institute, Zhuhai, Guangdong, 519000, China.

AUTHOR INFORMATION

[a] These two authors contribution equally to this work

* Corresponding authors:

Prof. Dr. Yun Ling, E-mail address: yunling@fudan.edu.cn

Prof. Dr. Yaming Zhou, E-mail address: ymzhou@fudan.edu.cn

Scheme S1. A schematic illustration of the procedure for N-linked glycans enrichment.

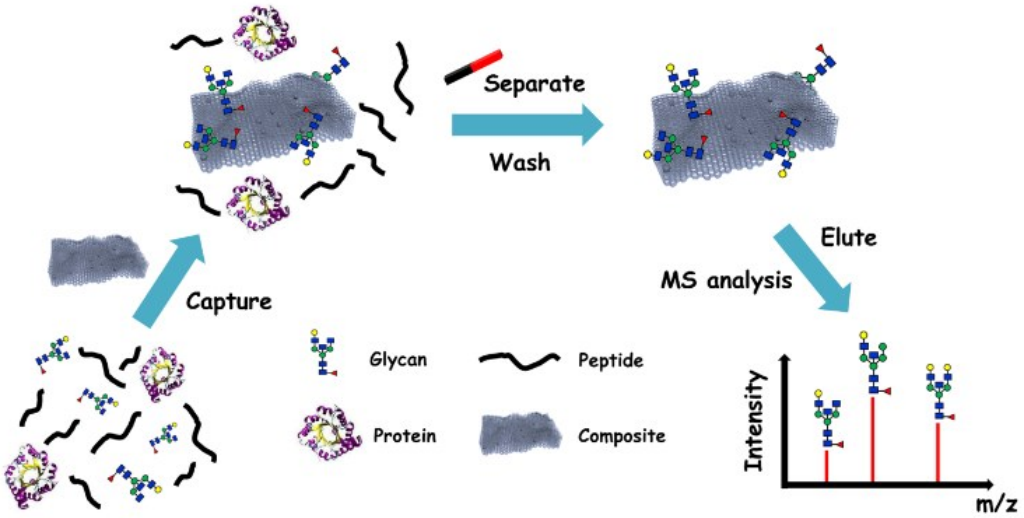

Fig. S1. (a) PXRD patterns of MagOG, MagOG@PF, MagOG@PF@Ni-MOF and Ni-MOF. The red star symbol labels diffraction peak of graphene nanoplatelets, and green triangle labels the diffraction peaks of Fe_3O_4 nanoparticles; (b) FT-IR spectra of MagOG, MagOG@PF, and MagOG@PF@Ni-MOF. The FT-IR spectrum provides additional evidence of the formation of PF layer because of the presence of new absorption bands in the range of 1560-950 cm^{-1} attributing to the stretching and plane bending vibration of the aromatic rings. Moreover, the sharp increase in intensity of the peaks at 3430 cm^{-1} is resulted from the O-H stretching vibration of PF resin. The FT-IR spectrum of MagOG@PF@Ni-MOF also reveals difference. Besides the intensity of the peaks at 3430 cm^{-1} and 1560-950 cm^{-1} increasing, a new peak appears at 778 cm^{-1} belonging to the substituted aromatic compounds, indicating that the existence of the organic ligand 1H-pyrazole-4-carboxylic acid.

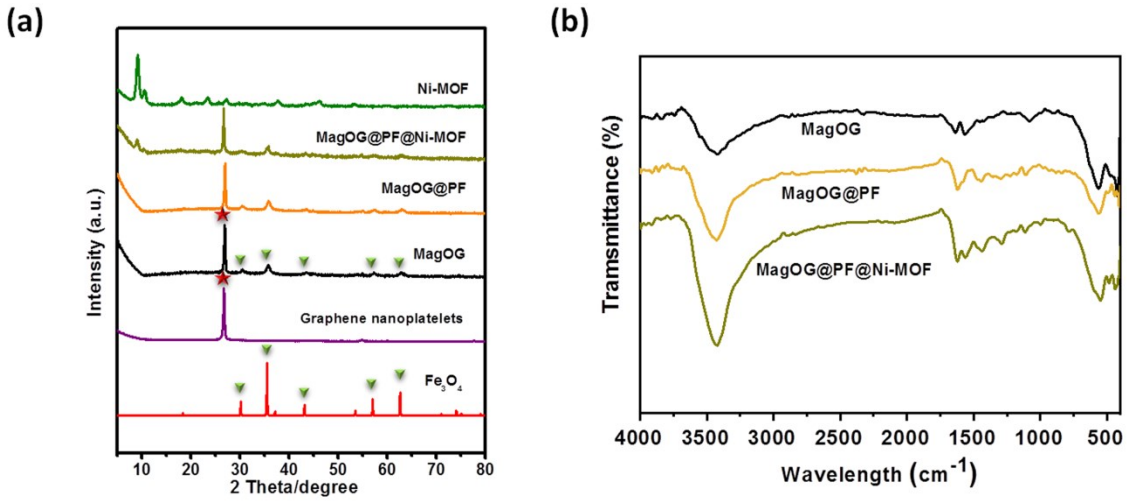

Fig. S2. PXRD patterns of FeNi-G/PC-600, 700, 800, and 900, in which the red star labels the diffraction peak of graphene nanoplatelets, the green triangle labels the diffraction peaks of Fe_3O_4, the red ball represents the formation of FeNi at T = 600 °C.

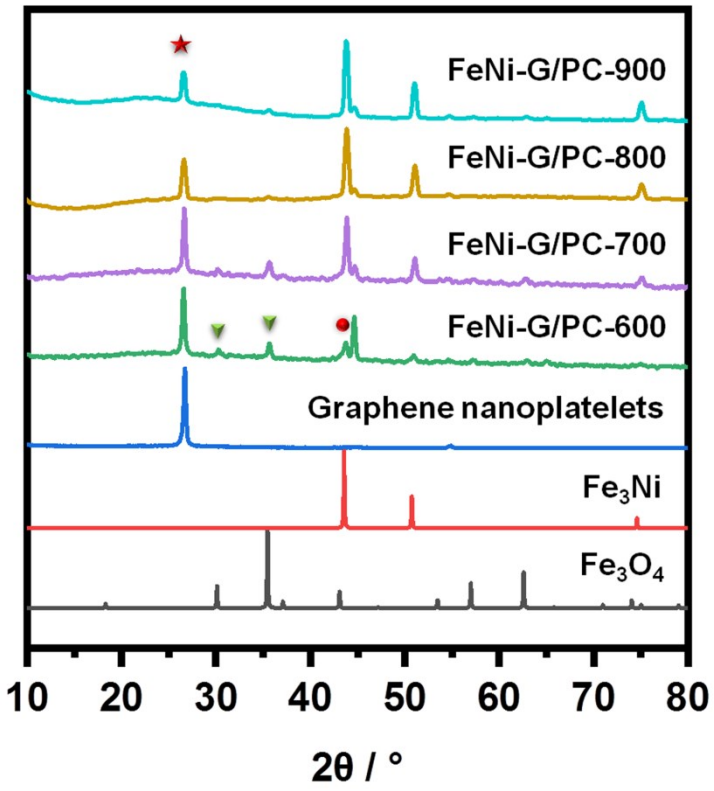

Fig. S3. PXRD pattern of MagOG@PF (a) and Ni-MOF (b) carbonized at T = 800 °C, showing the generation Fe phase labels as blue triangle (the green triangle labels the diffraction peaks of Fe_3O_4) and the Ni phase labels as green cubic.

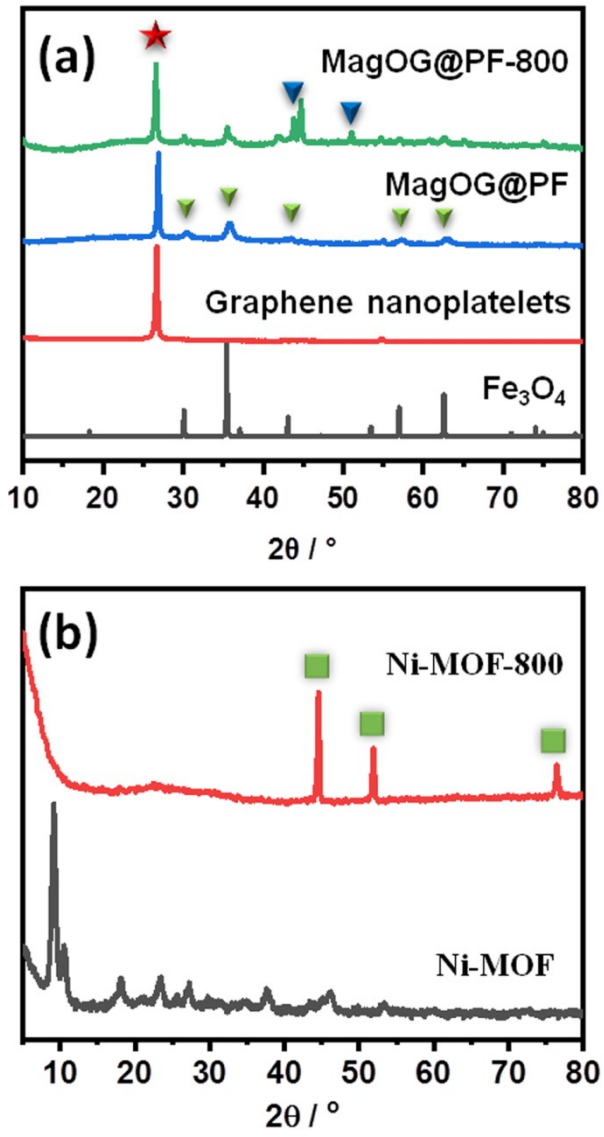

Fig. S4. N_2 adsorption-desorption isotherms of MagOG@PF@Ni-MOF at 77 K. Pore size distributions calculated by H-K for the analysis of micropore and BJH for the mesopore.

The result demonstrate that the Brunauer-Emmett-Teller (BET) surface area of MagOG@PF@Ni-MOF is 62 m^2/g. Analysis of pore size distribution based on adsorption isotherm by H-K method indicates a mean diameter of ~18Å (Fig S4b). Analysis of pore size distribution based on desorption isotherm by BJH method reveals a mean diameter of ~4 nm (Fig S4c).

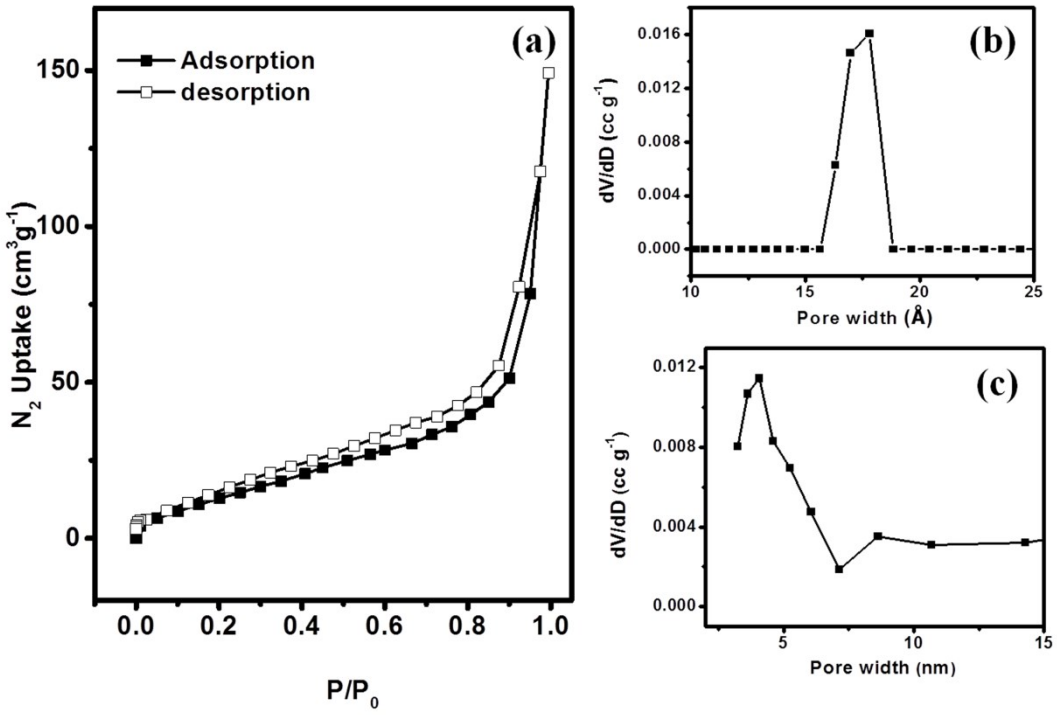

Fig. S5. Magnetization curve of composites at 300K. Field-dependent magnetic study is carried out to access the magnetic property of MagOG, MagOG@PF@Ni-MOFand FeNi-G/PC-800 at 300 K, respectively (Fig S5). M-H plot shows that the saturation magnetization (Ms) of MagOG, MagOG@PF@Ni-MOFand FeNi-G/PC-800 are 35.1 emu/g, 24.5 emu/g and 32.6 emu/g respectively.

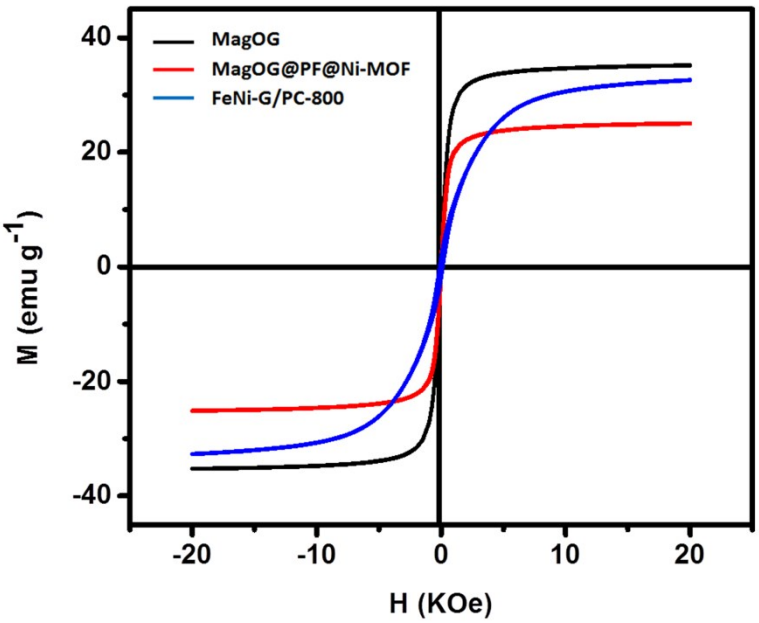

Fig. S6. N_2 adsorption-desorption isotherms of FeNi-G/PC-T (T=700, 800, 900) at 77 K. Pore size distributions calculated by H-K for the analysis of micropore and BJH for the mesopore, respectively.

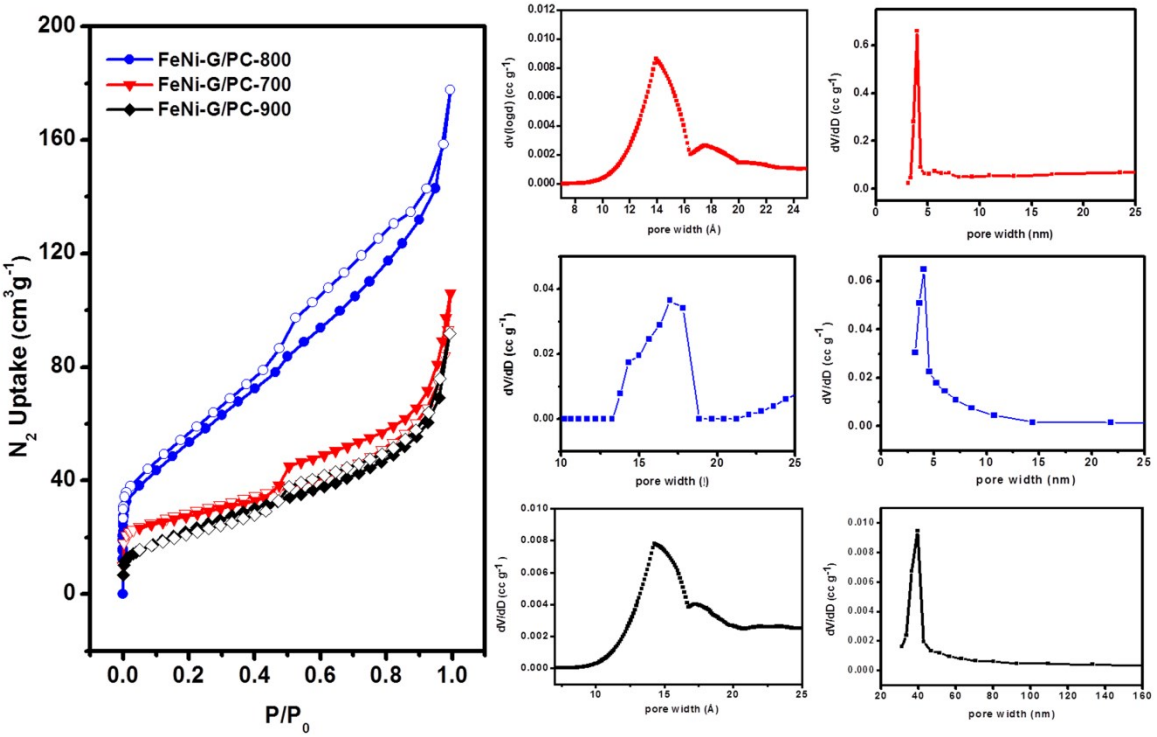

Fig. S7. Raman spectrum of FeNi-G/PC-T (T = 600, 700, 800, 900 °C).

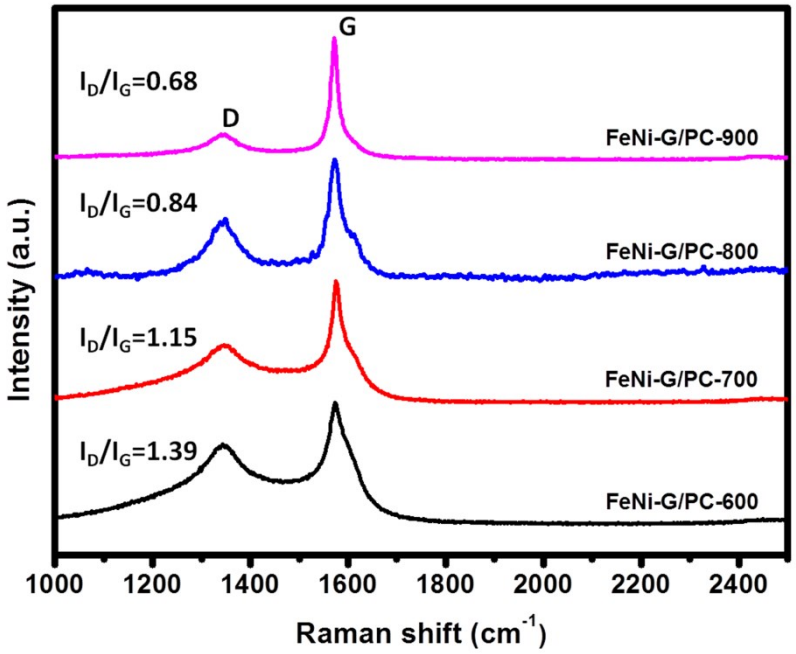

Fig. S8. MALDI-TOF-MS analysis of glycans derived from OVA enriched by FeNi-G/PC-800 with different eluent (a) 10% ACN; (b) 30% ACN; (c) 50% ACN and (d) 80% ACN. The peaks marked with red asterisks represent the identified N-linked glycans.

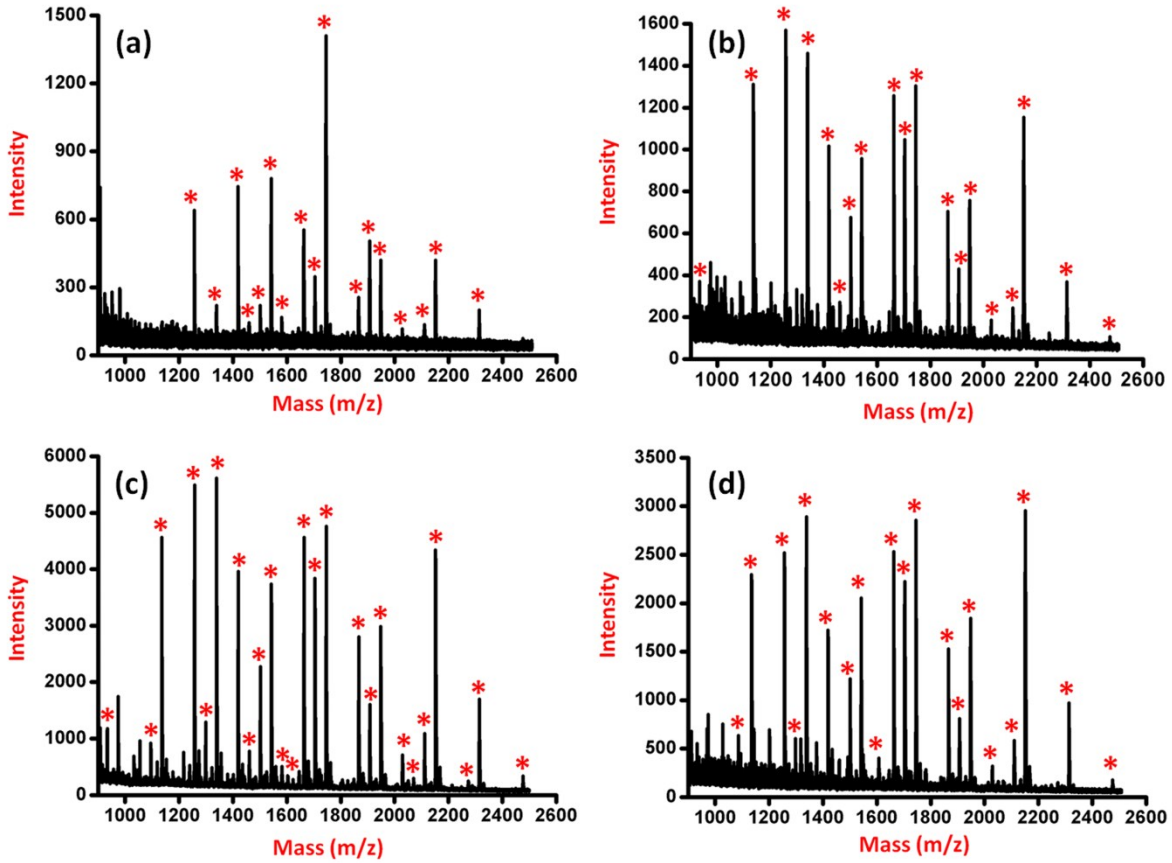

Fig. S9. MALDI-TOF-MS analysis of the N-linked glycans derived from the mixture of OVA digests, glycosylated proteins (OVA), and nonglycosylated proteins (BSA) (at mass ratio of 1:800:800). Supernate before enrichment (a) in positive mode and (b) in linear mode and eluate after enrichment by FeNi-G/PC-800 (c) in positive mode and (d) in linear mode. The peaks marked with red asterisks represent the identified N-linked glycans.

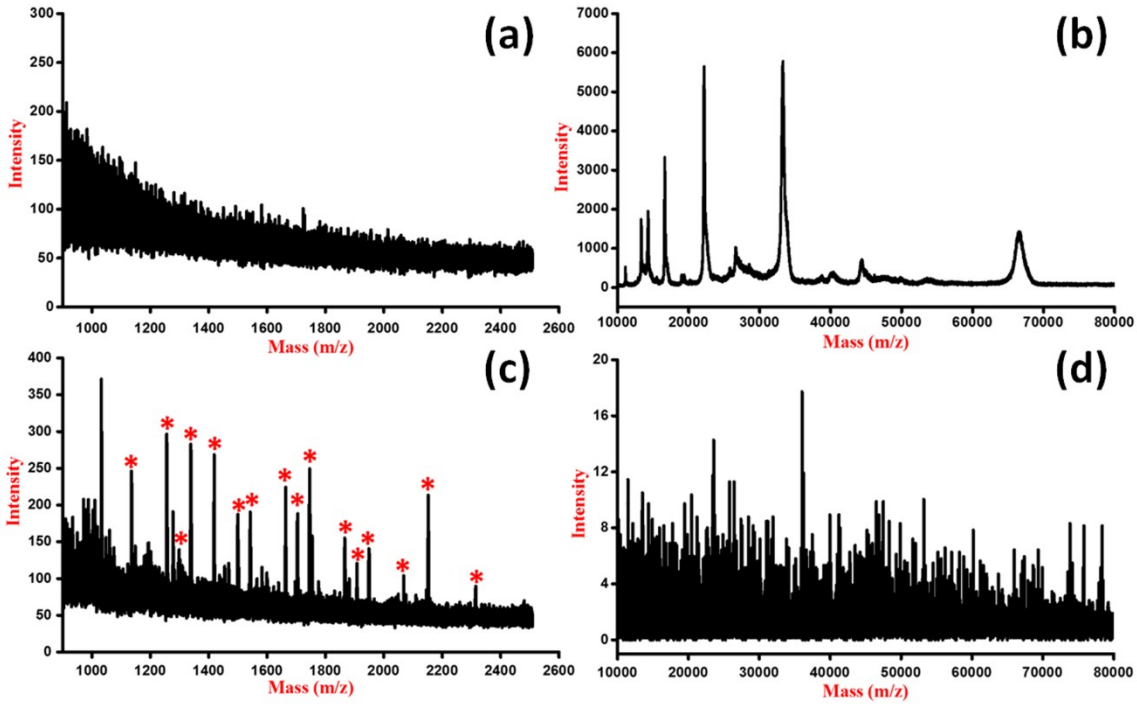

Fig. S10. MALDI-TOF-MS analysis of N-linked glycans identified from normal human serum before enrichment with FeNi-G/PC-800.

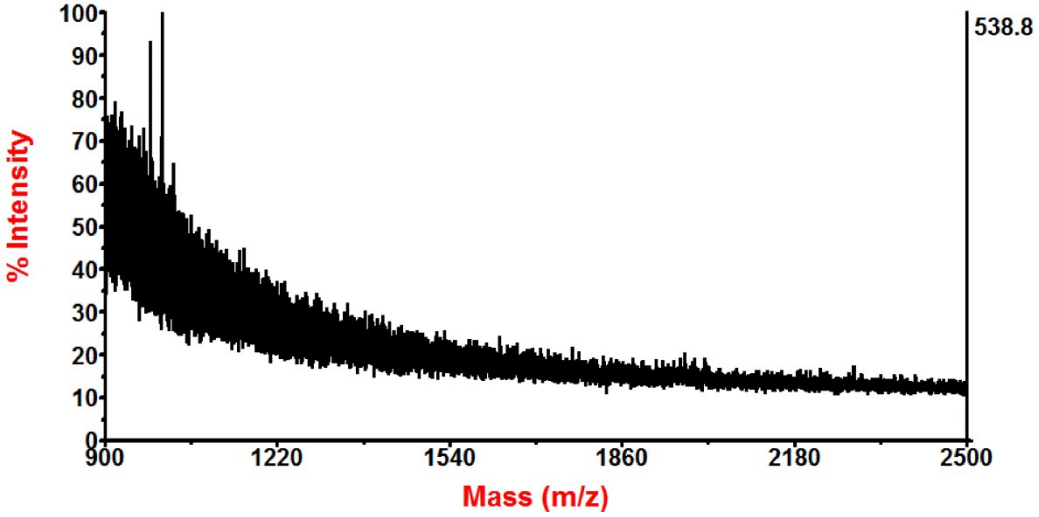

Detailed information of N-linked glycans.

Table S1 List of identified 25 N-linked glycans released from OVA digests enriched by FeNi-G/PC-800.

No.	M/Z $[M+Na]^+$	S/N	Composition
1	933.4	126.88	$Hex_3HexNAc_2$
2	1095.4	91.01	$Hex_4HexNAc_2$
3	1136.5	553.22	$Hex_3HexNAc_3$
4	1257.5	670.13	$Hex_5HexNAc_2$
5	1298.6	151.13	$Hex_4HexNAc_3$
6	1339.6	775.46	$Hex_3HexNAc_4$
7	1419.6	507.42	$Hex_6HexNAc_2$
8	1460.7	89.87	$Hex_5HexNAc_3$
9	1501.7	309.93	$Hex_4HexNAc_4$
10	1542.7	522.08	$Hex_3HexNAc_5$
11	1581.7	51.14	$Hex_7HexNAc_2$
12	1622.7	21.61	$Hex_6HexNAc_3$
13	1663.8	557.08	$Hex_5HexNAc_4$
14	1704.8	521.13	$Hex_4HexNAc_5$
15	1745.8	676.91	$Hex_3HexNAc_6$
16	1866.9	387.13	$Hex_5HexNAc_5$
17	1907.0	227.13	$Hex_4HexNAc_6$
18	1948.0	436.89	$Hex_3HexNAc_7$
19	2028.0	84.22	$Hex_6HexNAc_5$
20	2069.1	20.38	$Hex_5HexNAc_6$
21	2110.1	158.60	$Hex_4HexNAc_7$
22	2151.1	728.90	$Hex_8HexNAc_4$
23	2272.2	25.52	$Hex_4HexNAc_7$
24	2313.2	301.87	$Hex_3HexNAc_8$
25	2475.3	46.40	$Hex_5HexNAc_8$

Table S2. Detailed information of the observed N-linked glycans from normal human serum by enriching with FeNi-G/PC-800 composites (N-linked glycans were released by PNGase F digestion, and glycan strcutures were searched from Glycoworkbench through the Mol. wt of oligosaccharide. Part of the strcutures has been demonstrated.

No	M/Z ($[M+nNa]^+$)	Composition	Structure (M)
1	933.1	H3N2	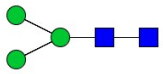
2	1136.4	H3N3	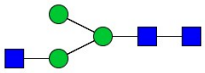
3	1257.4	H5N2	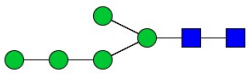
4	1281.5	H3N3F1	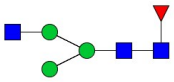
5	1298.5	H4N3	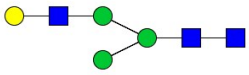
6	1338.5	H3N4	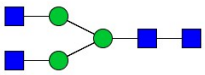
7	1388.9	H5N2X1	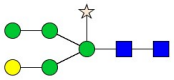
8	1419.5	H6N2	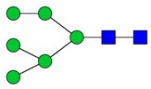
9	1443.5	H4N3F1	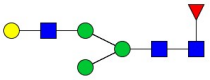
10	1460.5	H5N3	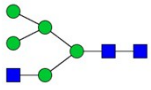
11	1485.6	H3N4F1	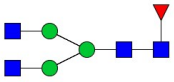
12	1501.6	H4N4	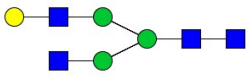

13	1541.6	H3N5	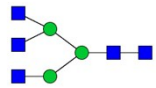
14	1581.6	H7N2	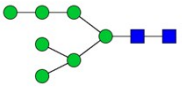
15	1606.2	H5N3F1	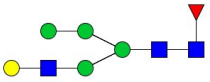
16	1621.6	H6N3	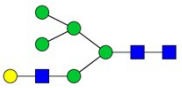
17	1629.6	H3N4A1	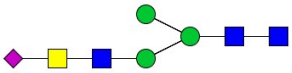
18	1646.7	H4N4F1	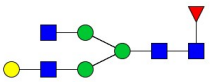
19	1662.7	H5N4	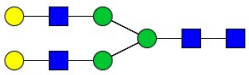
20	1688.7	H3N5F1	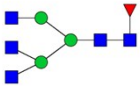
21	1704.7	H4N5	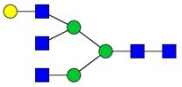
22	1743.6	H8N2	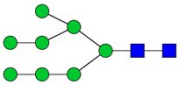
23	1767.6	H6N3F1	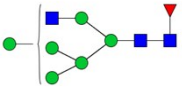
24	1791.7	H3N5A1	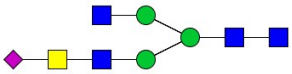
25	1808.7	H5N4F1	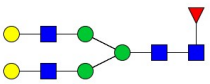
26	1814.2	H4N4A1	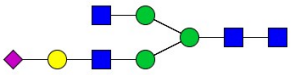
27	1824.6	H6N4	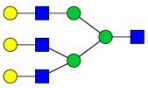
28	1850.7	H4N5F1	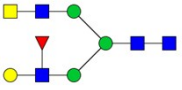

29	1865.7	H5N5	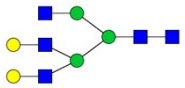
30	1905.2	H9N2	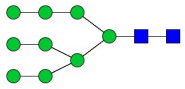
31	1925.7	H4N45F2X1	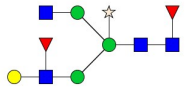
32	1954.5	H5N4A1	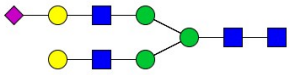
33	2012.8	H5N5F1	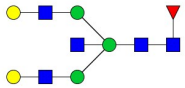
34	2028.8	H6N5	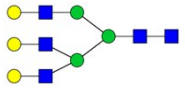
35	2156.8	H5N5A1	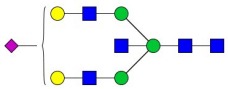
36	2173.8	H6N5F1	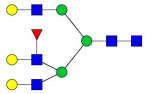
37	2188.6	H5N3F1A2	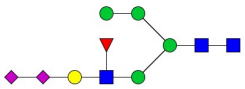
38	2221.7	H6N3A2	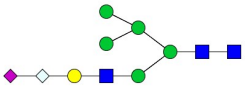
39	2245.7	H5N4A2	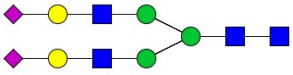
40	2267.7	H5N4F2A1	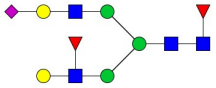
41	2282.7	H5N5F1A1	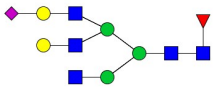
42	2288.8	H5N4A2	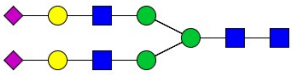
43	2294.7	H7N4A1	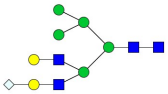
44	2302.7	H4N5A2	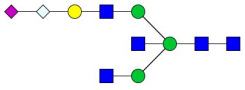

45	**2305.7**	**H5N5F3**	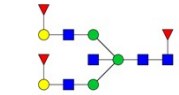
46	**2326.8**	**H5N5F1A1**	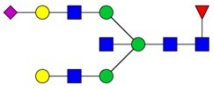
47	**2340.8**	**H6N5A1**	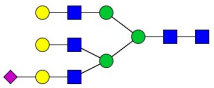
48	**2361.8**	**H6N5A1**